Journal of Applied Analysis and Computation
Volume 17, Number 1, February 2027, 473–499
Website:http://www.jaac-online.com
DOI:10.11948/20260064

A CAPUTO FRACTIONAL LOTKA-VOLTERRA MODEL FOR COMPETITIVE OPINION DYNAMICS: STABILITY ANALYSIS AND DATA-DRIVEN VALIDATION

Muath Awadalla[1] and Abulrahman A. Sharif[2,3,†]

Abstract Competitive opinion dynamics in socio-economic systems often exhibit memory and history-dependent interactions that cannot be adequately captured by classical integer-order models. In this paper, we propose a Caputo fractional-order Lotka-Volterra framework to describe the competition between two interacting opinions and provide a rigorous mathematical analysis of the resulting system. By reformulating the model in an equivalent Volterra integral form, we establish existence and uniqueness of solutions and conduct a local stability analysis based on the Jacobian matrix and the Matignon criterion.The analysis shows that the coexistence equilibrium is asymptotically stable for $0 < q < 1$ and neutrally stable for the classical case $q = 1$.The theoretical findings are supported by numerical simulations using a predictor-corrector Adams-Bashforth-Moulton scheme for Caputo fractional differential equations. Furthermore, an illustrative calibration based on normalized pseudo-temporal prevalence data and least-squares fitting demonstrates that the fractional model achieves a lower root-mean-square error compared to its classical counterpart, which is consistent with the memory-induced damping mechanism predicted by the stability analysis. In response to reviewer comments, we emphasize that the empirical component is purely illustrative: The data lack genuine timestamps, and no claim of statistical significance or predictive validation is made.

Keywords Caputo fractional derivative, fractional Lotka-Volterra model, opinion dynamics, stability analysis, Matignon criterion, illustrative calibration.

MSC(2010) 26A33, 34A08, 37C75, 91D30, 93D20.

1. Introduction

The rapid expansion of the platform economy has fundamentally reshaped socio-economic interactions, transforming digital platforms into large-scale ecosystems where transactions, information exchange, and opinion formation are deeply intertwined [13, 23, 43]. In such environments, user engagement and collective behavior emerge from complex interaction mechanisms that resemble dynamical systems studied in physics and applied mathematics [7, 14, 17, 48]. The foundational works in sociophysics and statistical physics of social dynamics, including the classical Ising model [20], voter-type models [9], and population-interaction frameworks inspired by

[†]The corresponding author.
[1]Department of Mathematics and Statistics, College of Science, King Faisal University, Al Ahsa 31982, Saudi Arabia
[2]Department of Mathematics, Hodeidah University, AL-Hudaydah, Yemen
[3]Department of Mathematics, Dr. Babasaheb Ambedkar Marathwada University Chh. Sambhajinagar 431004, Maharashtra, India
Email: mawadalla@kfu.edu.sa(M. Awadalla), maths.ahs@bamu.ac.in(A. A. Sharif)

Lotka and Volterra [28, 51], have provided essential mathematical tools for modeling competition, consensus, and coexistence phenomena. Over time, these classical frameworks have been extended beyond biology to technological competition, market diffusion, and socio-economic forecasting [35, 36, 38]. Their appeal lies in their interpretability and tractable dynamical structure.

However, a fundamental limitation persists: Most classical formulations rely on integer-order differential equations, implying Markovian dynamics where the system's future evolution depends only on its present state. This assumption is often unrealistic in platform-based contexts, where behavioral inertia, memory, delayed adaptation, and historical exposure influence collective evolution, and where temporal-network effects play a crucial role [8, 18, 34]. Fractional calculus provides a mathematically rigorous framework for incorporating memory effects into dynamical systems [24, 31, 32, 39, 44]. Unlike integer-order derivatives, which are local operators, fractional derivatives are nonlocal and naturally incorporate a weighted history of the state variable. Specifically, the Caputo fractional derivative of order $q \in (0,1]$ involves a convolution kernel $(t-s)^{-q}$, which decays as a power law rather than exponentially.

This power-law memory structure is particularly relevant for opinion dynamics. More generally, power-law kernels are widely used to represent long-memory effects in complex systems and provide a mathematically consistent framework for incorporating persistence and delayed responses into social interaction models [18, 34]. Thus, fractional derivatives offer a principled way to model long-range dependencies in collective behavioral dynamics.

Recent advances in fractional calculus have been applied to diverse fields including epidemic modeling [5], virus propagation [3], optimal control of nonlinear systems [49], and chaotic system analysis [40, 50]. Analytical techniques for variable-order fractional systems have also been developed [1], while numerical methods for fractal-fractional derivatives continue to evolve [4]. Within social dynamics, fractional-order models have been proposed for rumor spreading [45], crowd dynamics [6], and population interactions [21]. Nevertheless, most existing fractional opinion models focus on single-population or network-based spreading without a rigorous stability analysis of competitive coexistence equilibria. The present work addresses this gap by proposing a Caputo fractional-order Lotka-Volterra framework for competitive opinion dynamics between two interacting populations.

The main contributions of this paper are threefold. First, we provide a complete analytical treatment of the fractional system, including existence and uniqueness of solutions via a contraction mapping argument on the equivalent Volterra integral formulation, and positivity (invariance of the nonnegative quadrant) using a comparison principle for scalar Caputo inequalities. Second, we conduct a rigorous local stability analysis based on the Jacobian linearization and the Matignon criterion [33]. We show that the trivial equilibrium $E_0 = (0,0)$ is unstable for all $q \in (0,1]$, while the coexistence equilibrium $E^* = (d/c, a/b)$ satisfies: For $0 < q < 1$, it is locally asymptotically stable; for the classical case $q = 1$, it is neutrally stable (center-type).

This demonstrates that fractional memory changes the local stability character of the coexistence equilibrium from neutral stability in the classical case to local asymptotic stability for $0 < q < 1$.

Third, we support the theoretical findings with numerical simulations using the predictor-corrector Adams-Bashforth-Moulton scheme for Caputo fractional differential equations [11, 15]. The simulations illustrate that decreasing the fractional order q increases the damping effect. Furthermore, we provide an illustrative calibration using pseudo-temporal prevalence data from a publicly available Twitter dataset (Google vs. Microsoft). In response to reviewer comments, we emphasize that this calibration is **purely illustrative** and not a genuine data-driven validation: The dataset lacks genuine timestamps, and the pseudo-temporal aggregation is heuristic. The fractional model yields a modest reduction in root-mean-square error compared to the classical model, consistent with the memory-induced damping mechanism, but no claim of statistical significance or empirical superiority is made.

The remainder of this paper is organized as follows. Section 2 presents the fractional Lotka-Volterra model, its equivalent Volterra integral formulation, and proofs of existence, uniqueness, and positivity. Section 3 provides the stability analysis of the equilibrium points, including the Matignon-based linearization, eigenvalue analysis, positivity, continuation, and local stability properties. Section 4 describes the numerical method (Adams-Bashforth-Moulton scheme) and presents simulation results for different fractional orders. Section 5 offers an illustrative calibration of the model using pseudo-temporal prevalence data, together with a detailed discussion of limitations. Section 6 concludes the paper and outlines future research directions.

2. Mathematical model and theoretical foundations

2.1. Model formulation and preliminaries

The classical (integer–order) Lotka–Volterra type model for two competing opinions is

$$\frac{dx}{dt} = a\,x - b\,x\,y, \tag{2.1}$$

$$\frac{dy}{dt} = -d\,y + c\,x\,y, \tag{2.2}$$

where $x(t)$ and $y(t)$ denote the prevalences of Opinion A and Opinion B at time t, respectively. The constants $a, b, c, d > 0$ represent: Intrinsic growth of x, inhibition of x due to interaction with y, growth of y fueled by interaction with x, and intrinsic decay of y, respectively.

To incorporate memory effects, we replace the first–order derivatives by *Caputo fractional derivatives* of order $q \in (0, 1]$ (we intentionally reserve a for the growth parameter to avoid the common ambiguity of using α both as a parameter and as a fractional order).

Definition 2.1 (Caputo fractional derivative [44])**.** Let $q > 0$, $n = \lceil q \rceil$, and $f \in AC^n([0, T])$. The Caputo derivative of order q is defined by

$${}^{C}D^{q} f(t) = \frac{1}{\Gamma(n-q)} \int_0^t (t-s)^{n-q-1} f^{(n)}(s)\, ds. \tag{2.3}$$

In particular, if $q \in (0, 1]$, then $n = 1$ and (2.3) reduces to

$${}^{C}D^{q} f(t) = \frac{1}{\Gamma(1-q)} \int_0^t (t-s)^{-q} f'(s)\, ds. \tag{2.4}$$

The proposed fractional opinion dynamics model is therefore

$${}^{C}D^{q} x(t) = a\,x(t) - b\,x(t)\,y(t), \tag{2.5}$$

$${}^{C}D^{q} y(t) = -d\,y(t) + c\,x(t)\,y(t), \qquad t > 0, \tag{2.6}$$

subject to

$$x(0) = x_0 \geq 0, \qquad y(0) = y_0 \geq 0. \tag{2.7}$$

2.2. Equivalent Volterra integral formulation

We recall the fractional integral operator of order $q > 0$:

$$(I^q g)(t) := \frac{1}{\Gamma(q)} \int_0^t (t-s)^{q-1} g(s)\, ds.$$

For $q \in (0, 1]$ and sufficiently regular f, one has the identity

$$I^q\, {}^C D^q f(t) = f(t) - f(0). \tag{2.8}$$

Lemma 2.1 (Integral form)**.** *Let $q \in (0, 1]$ and assume $x, y \in C([0, T])$. Then (x, y) solves (2.5)–(2.6) with (2.7) on $[0, T]$ if and only if (x, y) satisfies the Volterra system*

$$x(t) = x_0 + \frac{1}{\Gamma(q)} \int_0^t (t-s)^{q-1}\, x(s)\big(a - b\, y(s)\big)\, ds, \tag{2.9}$$

$$y(t) = y_0 + \frac{1}{\Gamma(q)} \int_0^t (t-s)^{q-1}\, y(s)\big(-d + c\, x(s)\big)\, ds. \tag{2.10}$$

Proof. (*Fractional differential form $\Rightarrow$ integral form*). Assume (2.5) holds. Apply I^q to both sides and use (2.8):

$$I^q\, {}^C D^q x(t) = I^q[x(t)(a - b\, y(t))] \quad \Longrightarrow \quad x(t) - x(0) = \frac{1}{\Gamma(q)} \int_0^t (t-s)^{q-1} x(s)(a - b\, y(s))\, ds.$$

Since $x(0) = x_0$, we obtain (2.9). The same steps yield (2.10).

(*Integral form $\Rightarrow$ fractional differential form*). Conversely, assume (2.9)–(2.10) hold. Apply ${}^C D^q$ to (2.9). The Caputo derivative of the constant x_0 is zero, and ${}^C D^q I^q g(t) = g(t)$ for continuous g (see, e.g., [44]), giving

$${}^C D^q x(t) = x(t)(a - b\, y(t)).$$

Likewise, ${}^C D^q y(t) = y(t)(-d + c\, x(t))$, hence (2.5)–(2.6) hold. □

2.3. Local existence and uniqueness (well-posedness)

Define the vector field $F : \mathbb{R}^2 \to \mathbb{R}^2$ by

$$F(x, y) = \big(x(a - by),\, y(-d + cx)\big).$$

Note that F is locally Lipschitz on $\mathbb{R}^2$ (indeed, it is C^∞).

Theorem 2.1 (Local existence and uniqueness)**.** *Let $q \in (0, 1]$ and $(x_0, y_0) \in \mathbb{R}^2$. There exists $T > 0$ such that the fractional IVP (2.5)–(2.6) with (2.7) admits a unique solution $(x, y) \in C([0, T]; \mathbb{R}^2)$.*

Proof. We prove the result by a contraction mapping argument on the equivalent integral system (2.9)–(2.10).

Step 1. Functional setting. Let $B := C([0, T]; \mathbb{R}^2)$ with norm

$$\|(x, y)\|_B := \sup_{t \in [0,T]} |x(t)| + \sup_{t \in [0,T]} |y(t)|.$$

Fix $M > 0$ and define the closed ball around the initial data

$$\Omega := \Big\{(x,y) \in B : \sup_{t\in[0,T]} |x(t) - x_0| \le M,\ \sup_{t\in[0,T]} |y(t) - y_0| \le M\Big\}.$$

Then for any $(x,y) \in \Omega$ and $t \in [0,T]$ we have the uniform bounds

$$|x(t)| \le K_x := |x_0| + M, \qquad |y(t)| \le K_y := |y_0| + M.$$

Step 2. Define the Picard operator. Define $\Phi : \Omega \to B$ by $\Phi(x,y) = (\Phi_1(x,y), \Phi_2(x,y))$ where

$$\Phi_1(x,y)(t) := x_0 + \frac{1}{\Gamma(q)} \int_0^t (t-s)^{q-1}\, x(s)\big(a - b\, y(s)\big)\, ds,$$
$$\Phi_2(x,y)(t) := y_0 + \frac{1}{\Gamma(q)} \int_0^t (t-s)^{q-1}\, y(s)\big(-d + c\, x(s)\big)\, ds.$$

A fixed point of Φ is exactly a solution of (2.9)–(2.10).

Step 3. Φ maps Ω into itself for small T. For $(x,y) \in \Omega$ and any $t \in [0,T]$,

$$\begin{aligned}|\Phi_1(x,y)(t) - x_0| &\le \frac{1}{\Gamma(q)} \int_0^t (t-s)^{q-1}\, |x(s)|\big(|a| + b|y(s)|\big)\, ds \\ &\le \frac{K_x(|a| + bK_y)}{\Gamma(q)} \int_0^t (t-s)^{q-1}\, ds.\end{aligned}$$

Using $\int_0^t (t-s)^{q-1} ds = t^q/q$ and $\Gamma(q+1) = q\Gamma(q)$ yields

$$|\Phi_1(x,y)(t) - x_0| \le \frac{K_x(|a| + bK_y)}{\Gamma(q+1)}\, t^q \le \frac{K_x(|a| + bK_y)}{\Gamma(q+1)}\, T^q.$$

Similarly,

$$|\Phi_2(x,y)(t) - y_0| \le \frac{K_y(|d| + cK_x)}{\Gamma(q+1)}\, T^q.$$

Hence, if $T > 0$ is chosen such that

$$\frac{K_x(|a| + bK_y)}{\Gamma(q+1)}\, T^q \le M \quad \text{and} \quad \frac{K_y(|d| + cK_x)}{\Gamma(q+1)}\, T^q \le M,$$

then $\Phi(x,y) \in \Omega$. This is possible for sufficiently small T.

Step 4. Φ is a contraction on Ω for small T. Let $(x_1,y_1), (x_2,y_2) \in \Omega$. For $t \in [0,T]$,

$$\begin{aligned}&|\Phi_1(x_1,y_1)(t) - \Phi_1(x_2,y_2)(t)| \\ \le &\frac{1}{\Gamma(q)} \int_0^t (t-s)^{q-1} \big|x_1(s)(a - by_1(s)) - x_2(s)(a - by_2(s))\big|\, ds \\ \le &\frac{1}{\Gamma(q)} \int_0^t (t-s)^{q-1} \Big(|a|\, |x_1(s) - x_2(s)| + b|x_1(s)y_1(s) - x_2(s)y_2(s)|\Big)\, ds.\end{aligned}$$

Now,

$$|x_1y_1 - x_2y_2| = |x_1(y_1 - y_2) + y_2(x_1 - x_2)|$$

$$\begin{aligned}&\le |x_1|\,|y_1-y_2| + |y_2|\,|x_1-x_2|\\&\le K_x|y_1-y_2| + K_y|x_1-x_2|.\end{aligned}$$

Therefore,

$$\begin{aligned}|\Phi_1(x_1,y_1)(t)-\Phi_1(x_2,y_2)(t)| \le{}& \frac{|a|+bK_y}{\Gamma(q)}\int_0^t (t-s)^{q-1}|x_1(s)-x_2(s)|\,ds\\&+\frac{bK_x}{\Gamma(q)}\int_0^t (t-s)^{q-1}|y_1(s)-y_2(s)|\,ds.\end{aligned}$$

Taking suprema over $t\in[0,T]$ and using $\int_0^t (t-s)^{q-1}ds = t^q/q = \frac{t^q}{\Gamma(q+1)}\Gamma(q)$ gives

$$\begin{aligned}&\sup_{t\in[0,T]} |\Phi_1(x_1,y_1)(t)-\Phi_1(x_2,y_2)(t)|\\&\le \frac{T^q}{\Gamma(q+1)}\Big((|a|+bK_y)\sup_t|x_1-x_2| + bK_x\sup_t|y_1-y_2|\Big).\end{aligned}$$

Similarly,

$$\begin{aligned}&\sup_{t\in[0,T]} |\Phi_2(x_1,y_1)(t)-\Phi_2(x_2,y_2)(t)|\\&\le \frac{T^q}{\Gamma(q+1)}\Big(cK_y\sup_t|x_1-x_2| + (|d|+cK_x)\sup_t|y_1-y_2|\Big).\end{aligned}$$

Adding the two inequalities yields

$$\|\Phi(x_1,y_1)-\Phi(x_2,y_2)\|_B \le \frac{T^q}{\Gamma(q+1)}\,L\,\|(x_1,y_1)-(x_2,y_2)\|_B,$$

where one may take

$$L := (|a|+bK_y) + bK_x + cK_y + (|d|+cK_x).$$

Choose $T>0$ additionally small so that $\frac{T^q}{\Gamma(q+1)}L<1$. Then Φ is a contraction on Ω.

Step 5. Conclude by Banach's fixed point theorem. Since Ω is complete (as a closed subset of a Banach space) and Φ is a contraction mapping Ω into itself, Φ has a unique fixed point in Ω. By Lemma 2.1, this fixed point is the unique solution of (2.5)–(2.6) on $[0,T]$. □

2.4. Positivity (invariance of the nonnegative quadrant) and continuation

The next result provides a rigorous positivity statement that does *not* rely on the incorrect inequality argument "$x(t_1)\ge x_0$". The key idea is to compare x and y to scalar linear fractional equations with nonnegative Mittag–Leffler solutions.

Lemma 2.2 (A basic comparison fact). *Let $q\in(0,1]$ and let $u\in C([0,T])$ satisfy the integral inequality*

$$u(t)\ge u_0 - \frac{\kappa}{\Gamma(q)}\int_0^t (t-s)^{q-1}u(s)\,ds,\qquad t\in[0,T], \tag{2.11}$$

for some constants $u_0\ge 0$ and $\kappa\ge 0$. Then $u(t)\ge 0$ for all $t\in[0,T]$.

Proof. Define z as the unique solution of the linear Caputo problem

$$^{C}D^q z(t) = -\kappa z(t), \qquad z(0) = u_0.$$

Its explicit solution is

$$z(t) = u_0 E_q(-\kappa t^q) \geq 0, \qquad t \in [0, T],$$

since $E_q(-\kappa t^q)$ is completely monotone and nonnegative for $\kappa \geq 0$ and $q \in (0, 1]$. Equivalently, z satisfies

$$z(t) = u_0 - \frac{\kappa}{\Gamma(q)} \int_0^t (t-s)^{q-1} z(s)\, ds.$$

Consider $w(t) := u(t) - z(t)$. Subtracting the last identity from (2.11) gives

$$w(t) \geq -\frac{\kappa}{\Gamma(q)} \int_0^t (t-s)^{q-1} w(s)\, ds.$$

Define $m := \min_{t\in[0,T]} w(t)$ (it exists by continuity). If $m < 0$, pick t^* such that $w(t^*) = m$. Then the right-hand side at t^* satisfies

$$-\frac{\kappa}{\Gamma(q)} \int_0^{t^*} (t^* - s)^{q-1} w(s)\, ds \geq -\frac{\kappa}{\Gamma(q)} \int_0^{t^*} (t^* - s)^{q-1} m\, ds = -\kappa m \frac{(t^*)^q}{\Gamma(q+1)}.$$

Hence,

$$m = w(t^*) \geq -\kappa m \frac{(t^*)^q}{\Gamma(q+1)}.$$

Since the coefficient on the right is nonnegative, the inequality implies

$$m\Big(1 + \kappa \frac{(t^*)^q}{\Gamma(q+1)}\Big) \geq 0,$$

which is impossible if $m < 0$. Therefore $m \geq 0$ and thus $w(t) \geq 0$ for all t. Consequently $u(t) = z(t) + w(t) \geq 0$ for all $t \in [0, T]$. ☐

Theorem 2.2 (Positivity of solutions)**.** *Let $q \in (0, 1]$ and $(x_0, y_0) \in \mathbb{R}^2_{\geq 0}$. Let (x, y) be the (local) solution of* (2.5)–(2.6) *on $[0, T]$ given by Theorem 2.1. Then*

$$x(t) \geq 0, \qquad y(t) \geq 0, \qquad \forall\, t \in [0, T].$$

Proof. We work on the existence interval $[0, T]$.

Step 1. Positivity of x. Since y is continuous on $[0, T]$, it is bounded there; denote

$$M_y := \sup_{t\in[0,T]} y(t) \quad \text{(finite)}.$$

Then for all $t \in [0, T]$,

$$a - b\, y(t) \geq a - b\, M_y \geq -\kappa_x, \qquad \text{where } \kappa_x := \max\{0,\, bM_y - a\} \geq 0.$$

Using the integral form (2.9) and the bound above,

$$x(t) = x_0 + \frac{1}{\Gamma(q)} \int_0^t (t-s)^{q-1} x(s)\big(a - b\, y(s)\big)\, ds \geq x_0 - \frac{\kappa_x}{\Gamma(q)} \int_0^t (t-s)^{q-1} x(s)\, ds.$$

This is exactly (2.11) with $u = x$, $u_0 = x_0$ and $\kappa = \kappa_x$. By Lemma 2.2, we conclude $x(t) \geq 0$ for all $t \in [0, T]$.

Step 2. Positivity of y. Similarly, since x is continuous on $[0, T]$, let $M_x := \sup_{t\in[0,T]} x(t) < \infty$. Then for all $t \in [0, T]$,

$$-d + c\,x(t) \geq -d \geq -\kappa_y, \qquad \kappa_y := d \geq 0.$$

From (2.10) we obtain

$$y(t) \geq y_0 - \frac{\kappa_y}{\Gamma(q)} \int_0^t (t-s)^{q-1} y(s)\, ds,$$

and again Lemma 2.2 implies $y(t) \geq 0$ on $[0, T]$. □

Remark 2.1 (Continuation criterion; avoid overstating global boundedness)**.** Theorem 2.1 guarantees well-posedness on some $[0, T]$. Standard continuation theory for Caputo IVPs with locally Lipschitz right-hand side yields: There exists a maximal interval $[0, T_{\max})$ on which the solution is uniquely defined, and either $T_{\max} = +\infty$ (global solution) or $\|(x(t), y(t))\| \to +\infty$ as $t \uparrow T_{\max}$. Therefore, to claim global existence/boundedness for all $t \geq 0$, one must provide an *a priori* bound preventing blow-up. In this paper, we will explicitly state stability properties of equilibria (Section 3) and support the long-time behavior numerically.

3. Stability analysis of the equilibrium points

3.1. Preliminaries on fractional stability theory

We consider the Caputo fractional dynamical system of order $q \in (0, 1]$:

$$^{C}D^q \mathbf{X}(t) = \mathbf{F}(\mathbf{X}(t)), \qquad \mathbf{X}(0) = \mathbf{X}_0, \tag{3.1}$$

where $\mathbf{X}(t) \in \mathbb{R}^2$ and $\mathbf{F} \in C^1(\mathbb{R}^2, \mathbb{R}^2)$.

In contrast to integer-order systems, the local stability of fractional-order nonlinear systems is determined via linearization together with the spectral condition established by Matignon.

Theorem 3.1 (Fractional linearization principle)**.** *Let $\mathbf{F} \in C^1$ and let $\mathbf{X}^*$ be an equilibrium point of the fractional system $^{C}D^q\mathbf{X}(t) = \mathbf{F}(\mathbf{X}(t))$, $q \in (0, 1)$. If all eigenvalues λ_i of the Jacobian matrix $J(\mathbf{X}^*)$ satisfy*

$$|\arg(\lambda_i)| > \frac{q\pi}{2},$$

then $\mathbf{X}^*$ is locally asymptotically stable. Conversely, if at least one eigenvalue satisfies

$$|\arg(\lambda_i)| < \frac{q\pi}{2},$$

then the equilibrium is unstable.

This result follows from the Mittag-Leffler representation of solutions of linear fractional systems and the Hartman–Grobman-type theory for fractional differential equations.

3.2. Fractional opinion dynamics model

We analyze the fractional system introduced in Section 2:

$$^{C}D^q x(t) = a\,x(t) - b\,x(t)\,y(t), \tag{3.2}$$

$$ {}^{C}D^{q}y(t) = -d\,y(t) + c\,x(t)\,y(t), \tag{3.3} $$

where $a, b, c, d > 0$ and $q \in (0, 1]$.

Define

$$ \mathbf{F}(x, y) = \begin{pmatrix} f_1(x, y) \\ f_2(x, y) \end{pmatrix} = \begin{pmatrix} x(a - by) \\ y(-d + cx) \end{pmatrix}. $$

Since $\mathbf{F} \in C^{\infty}(\mathbb{R}^2)$, all requirements for local fractional linearization are satisfied.

3.3. Equilibrium points

Equilibrium points are obtained by solving

$$ f_1(x, y) = 0, \qquad f_2(x, y) = 0. $$

From

$$ f_1(x, y) = x(a - by) = 0, $$

we obtain

$$ x = 0 \quad \text{or} \quad y = \frac{a}{b}. $$

From

$$ f_2(x, y) = y(-d + cx) = 0, $$

we obtain

$$ y = 0 \quad \text{or} \quad x = \frac{d}{c}. $$

Theorem 3.2 (Equilibrium structure)**.** *The fractional system* (3.2)–(3.3) *admits exactly two non-negative equilibrium points in* $\mathbb{R}^2_{\geq 0}$*:*

$$ E_0 = (0, 0), \qquad E^{*} = \left(\frac{d}{c}, \frac{a}{b}\right). $$

Proof. If $x = 0$, then $f_2(0, y) = -dy = 0$, which implies $y = 0$, hence $E_0 = (0, 0)$. If $y = \frac{a}{b}$, substituting into $f_2 = 0$ gives

$$ -d\left(\frac{a}{b}\right) + cx\left(\frac{a}{b}\right) = 0 \quad \Rightarrow \quad \frac{a}{b}(-d + cx) = 0. $$

Since $a, b > 0$, we obtain $x = \frac{d}{c}$, which yields the interior equilibrium $E^{*} = \left(\frac{d}{c}, \frac{a}{b}\right)$. No other solutions exist in the non-negative quadrant. $\square$

3.4. Jacobian matrix and linearization

The Jacobian matrix is

$$ J(x, y) = \begin{pmatrix} \dfrac{\partial f_1}{\partial x} & \dfrac{\partial f_1}{\partial y} \\ \dfrac{\partial f_2}{\partial x} & \dfrac{\partial f_2}{\partial y} \end{pmatrix}. $$

Compute each entry explicitly:

$$ \frac{\partial f_1}{\partial x} = a - by, \qquad \frac{\partial f_1}{\partial y} = -bx, $$

$$\frac{\partial f_2}{\partial x} = cy, \qquad \frac{\partial f_2}{\partial y} = -d + cx.$$

Thus,

$$J(x, y) = \begin{pmatrix} a - by & -bx \\ cy & -d + cx \end{pmatrix}. \tag{3.4}$$

3.5. Stability of the trivial equilibrium $E_0 = (0, 0)$

Evaluating the Jacobian at E_0:

$$J(E_0) = \begin{pmatrix} a & 0 \\ 0 & -d \end{pmatrix}.$$

The eigenvalues are

$$\lambda_1 = a > 0, \qquad \lambda_2 = -d < 0.$$

Theorem 3.3 (Instability of E_0)**.** *The trivial equilibrium $E_0 = (0, 0)$ is unstable for all $q \in (0, 1]$.*

Proof. Since $\lambda_1 = a > 0$, we have

$$\arg(\lambda_1) = 0.$$

For fractional asymptotic stability, Matignon's condition requires

$$|\arg(\lambda_i)| > \frac{q\pi}{2}.$$

However,

$$|\arg(\lambda_1)| = 0 < \frac{q\pi}{2} \quad \forall q \in (0, 1].$$

Thus, the stability condition is violated, and the equilibrium is unstable. □

3.6. Stability of the coexistence equilibrium E^*

Evaluating the Jacobian at

$$E^* = \left(\frac{d}{c}, \frac{a}{b}\right),$$

we obtain

$$J(E^*) = \begin{pmatrix} a - b\frac{a}{b} & -b\frac{d}{c} \\ c\frac{a}{b} & -d + c\frac{d}{c} \end{pmatrix} = \begin{pmatrix} 0 & -\frac{bd}{c} \\ \frac{ac}{b} & 0 \end{pmatrix}.$$

3.7. Eigenvalue analysis at E^*

The characteristic polynomial is

$$\det(J(E^*) - \lambda I) = \begin{vmatrix} -\lambda & -\frac{bd}{c} \\ \frac{ac}{b} & -\lambda \end{vmatrix} = \lambda^2 + \frac{bd}{c} \cdot \frac{ac}{b} = \lambda^2 + ad.$$

Hence,

$$\lambda_{1,2} = \pm i\sqrt{ad}.$$

Therefore, the eigenvalues are purely imaginary conjugates with

$$|\arg(\lambda_{1,2})| = \frac{\pi}{2}.$$

Theorem 3.4. (Fractional stability of the interior equilibrium) *Let $q \in (0,1]$. The coexistence equilibrium*

$$E^* = \left(\frac{d}{c}, \frac{a}{b}\right)$$

satisfies:

1. *It is locally asymptotically stable for all $0 < q < 1$.*
2. *It is neutrally stable (center-type) when $q = 1$.*

Proof. The eigenvalues of the linearized system are $\lambda_{1,2} = \pm i\sqrt{ad}$, which satisfy

$$|\arg(\lambda_{1,2})| = \frac{\pi}{2}.$$

By Matignon's criterion, asymptotic stability requires

$$\frac{\pi}{2} > \frac{q\pi}{2} \quad \Longleftrightarrow \quad q < 1.$$

Thus, for all $0 < q < 1$, the equilibrium is locally asymptotically stable. When $q = 1$, the condition becomes equality, meaning the eigenvalues lie on the imaginary axis, which implies a center in the classical integer-order sense. This completes the rigorous stability classification. □

3.8. Qualitative properties: Positivity, continuation, and local stability

This subsection summarizes the qualitative properties that can be established rigorously for the fractional Lotka–Volterra opinion dynamics system. In view of the remarks raised by the reviewers, we deliberately avoid any claim of global attractivity or global boundedness that is not supported by a complete analytical proof. Throughout this subsection, we assume $a, b, c, d > 0$ and $q \in (0, 1]$.

3.8.1. Positive invariance of the nonnegative quadrant

The positivity result established in Section 2 immediately yields the following property.

Theorem 3.5 (Positive invariance)**.** *Let $(x_0, y_0) \in \mathbb{R}^2_{\geq 0}$. Then the unique solution of* (3.2)–(3.3) *satisfies*

$$x(t) \geq 0, \qquad y(t) \geq 0,$$

for every t in its interval of existence. Consequently, the nonnegative quadrant

$$\mathbb{R}^2_{\geq 0} := \{(x, y) \in \mathbb{R}^2 : x \geq 0,\ y \geq 0\}$$

is positively invariant.

Proof. The result follows directly from Theorem 2.2. □

3.8.2. A priori estimate and absence of finite-time blow-up

We introduce the auxiliary quantity

$$W(t) := x(t) + \frac{b}{c} y(t).$$

Since the Caputo derivative is linear, we obtain

$${}^{C}D^{q}W(t) = {}^{C}D^{q}x(t) + \frac{b}{c}\,{}^{C}D^{q}y(t).$$

Substituting the governing equations yields

$${}^{C}D^{q}W(t) = (ax - bxy) + \frac{b}{c}(-dy + cxy).$$

After cancellation of the mixed terms,

$${}^{C}D^{q}W(t) = ax - \frac{bd}{c}y.$$

Since $x(t) \geq 0$ and $y(t) \geq 0$, it follows that

$${}^{C}D^{q}W(t) \leq a\,x(t) \leq a\,W(t), \tag{3.5}$$

for all t in the interval of existence.

Lemma 3.1. *Let W satisfy (3.5) with $W(0) = W_0 \geq 0$. Then, for every finite $T > 0$,*

$$W(t) \leq W_0 E_q(at^q), \qquad 0 \leq t \leq T,$$

where $E_q(\cdot)$ denotes the Mittag–Leffler function.

Proof. Consider the scalar Caputo equation

$${}^{C}D^{q}z(t) = az(t), \qquad z(0) = W_0.$$

Its unique solution is

$$z(t) = W_0 E_q(at^q).$$

By the standard comparison principle for scalar Caputo fractional differential equations, inequality (3.5) together with the same initial condition implies

$$W(t) \leq z(t)$$

for all t in the common interval of existence. Therefore,

$$W(t) \leq W_0 E_q(at^q),$$

which completes the proof. □

Remark 3.1. The estimate above provides a rigorous bound on every finite interval $[0, T]$. In particular, it excludes finite-time blow-up and supports continuation of solutions on arbitrary finite time intervals.

However, because

$$E_q(at^q) \to \infty \qquad (t \to \infty,\ a > 0),$$

the estimate does not imply uniform boundedness as $t \to \infty$. Therefore, no claim of global boundedness is made in this work.

3.8.3. Observed trapping behavior

The numerical simulations reported in Section 4 indicate the existence of a practically relevant trapping region. Define

$$\mathcal{R} = \left[0, \frac{d}{c}\right] \times \left[0, \frac{a}{b}\right].$$

For all numerical experiments considered in this paper, trajectories starting from a variety of positive initial conditions eventually enter $\mathcal{R}$ and remain inside thereafter.

Remark 3.2. The above observation is purely numerical. A complete analytical proof that every positive trajectory enters $\mathcal{R}$, or that $\mathcal{R}$ is globally attracting, would require additional fractional comparison or Lyapunov-type arguments that are beyond the scope of the present work. Consequently, no such result is claimed here.

3.8.4. Local asymptotic stability of the coexistence equilibrium

The principal stability result of this paper has already been established in Theorem 3.4. Specifically, the coexistence equilibrium

$$E^* = \left(\frac{d}{c}, \frac{a}{b}\right)$$

is locally asymptotically stable for every fractional order $0 < q < 1$.

The proof relies on the eigenvalue structure of the Jacobian matrix and the Matignon stability criterion and does not require any Lyapunov construction.

3.8.5. Summary of rigorously established properties

The results proved in this section can be summarized as follows.

Theorem 3.6 (Rigorous qualitative properties)**.** *Let $a, b, c, d > 0$ and $0 < q < 1$. Then:*

1. *The nonnegative quadrant $\mathbb{R}^2_{\geq 0}$ is positively invariant.*
2. *Solutions do not exhibit finite-time blow-up.*
3. *The coexistence equilibrium*

$$E^* = \left(\frac{d}{c}, \frac{a}{b}\right)$$

is locally asymptotically stable.

Proof. Property (1) follows from Theorem 2.2.

Property (2) follows from Lemma 3.1 together with the standard continuation theorem for Caputo fractional differential equations (see, e.g., Diethelm [11]), which ensures that a local solution can be extended as long as it remains bounded on every finite interval.

Property (3) is exactly Theorem 3.4. □

Remark 3.3. A complete proof of global attractivity of E^* remains an open problem for the present model. Such a result would require substantially stronger analytical tools, for example a suitable fractional Lyapunov functional together with a strict decay estimate. Therefore, the present work restricts its conclusions to rigorously established local stability results and supporting numerical evidence.

4. Numerical simulations and results

The theoretical stability analysis established in Section 3 demonstrates that the long-term dynamics of the system depend critically on the fractional order $q \in (0, 1]$. In particular, the analysis showed that the coexistence equilibrium is neutrally stable in the classical integer-order case ($q = 1$), while it becomes locally asymptotically stable for all fractional orders $0 < q < 1$, in accordance with the Matignon stability criterion applied to the linearized system.

To illustrate these analytical findings and to provide further dynamical insight, we perform numerical simulations of the fractional-order model (3.2)–(3.3). Since closed-form solutions for nonlinear Caputo fractional differential equations are generally not available, a high-accuracy numerical scheme is employed to approximate the system trajectories and to examine the influence of the fractional memory parameter q on the transient and asymptotic behavior of the solutions.

4.1. Numerical method: Predictor–corrector Adams–Bashforth–Moulton scheme

To numerically solve the fractional-order system (3.2)–(3.3), we employ the predictor–corrector algorithm of the Adams–Bashforth–Moulton (ABM) type, which is one of the most reliable and widely used schemes for Caputo fractional differential equations [11].

This method is particularly suitable for nonlinear systems with Caputo derivatives due to its stability, convergence properties, and natural formulation through the equivalent Volterra integral representation established in Section 2.

4.1.1. Volterra integral formulation

Recall that the fractional system can be written in integral form as

$$x(t) = x_0 + \frac{1}{\Gamma(q)} \int_0^t (t-s)^{q-1} F_1(x(s), y(s))\, ds,$$

$$y(t) = y_0 + \frac{1}{\Gamma(q)} \int_0^t (t-s)^{q-1} F_2(x(s), y(s))\, ds,$$

where

$$F_1(x, y) = ax - bxy, \qquad F_2(x, y) = -dy + cxy,$$

and $q \in (0, 1]$ denotes the fractional order.

4.1.2. Time discretization

Let the computational interval be $[0, T]$ with a uniform step size $h = T/N$, and let

$$t_n = nh, \qquad n = 0, 1, \ldots, N.$$

The numerical approximations $(x_n, y_n) \approx (x(t_n), y(t_n))$ are computed iteratively using the predictor–corrector Adams–Bashforth–Moulton scheme described below.

For all simulations reported in this work, a sufficiently fine uniform mesh was employed to ensure numerical stability and convergence of the computed solutions. The same discretization strategy was used across all fractional orders considered in this section.

4.1.3. Predictor step (Explicit Adams–Bashforth)

The predictor values (x_{n+1}^P, y_{n+1}^P) are obtained using the fractional Adams–Bashforth formula:

$$x_{n+1}^P = x_0 + \frac{h^q}{\Gamma(q+1)} \sum_{j=0}^{n} b_{j,n+1} F_1(x_j, y_j),$$
$$y_{n+1}^P = y_0 + \frac{h^q}{\Gamma(q+1)} \sum_{j=0}^{n} b_{j,n+1} F_2(x_j, y_j),$$

where the coefficients $b_{j,n+1}$ are the fractional Adams weights defined by

$$b_{j,n+1} = (n+1-j)^q - (n-j)^q.$$

4.1.4. Corrector step (Implicit Adams–Moulton)

The predictor is then refined using the implicit Adams–Moulton corrector:

$$x_{n+1} = x_0 + \frac{h^q}{\Gamma(q+2)} \left[F_1(x_{n+1}^P, y_{n+1}^P) + \sum_{j=0}^{n} a_{j,n+1} F_1(x_j, y_j) \right],$$
$$y_{n+1} = y_0 + \frac{h^q}{\Gamma(q+2)} \left[F_2(x_{n+1}^P, y_{n+1}^P) + \sum_{j=0}^{n} a_{j,n+1} F_2(x_j, y_j) \right],$$

where the coefficients $a_{j,n+1}$ are given by

$$a_{j,n+1} = \begin{cases} n^{q+1} - (n-q)(n+1)^q, & j = 0, \\ (n-j+2)^{q+1} + (n-j)^{q+1} - 2(n-j+1)^{q+1}, & 1 \le j \le n, \\ 1, & j = n+1. \end{cases}$$

This predictor–corrector (PECE) procedure ensures improved accuracy and numerical stability for nonlinear fractional dynamical systems.

4.1.5. Accuracy and implementation

Under standard smoothness assumptions on F_1 and F_2, the global truncation error of the fractional Adams–Bashforth–Moulton scheme is of order $O(h^{1+q})$, which is consistent with the theoretical convergence results for Caputo fractional differential equations.

All simulations were implemented in MATLAB. To assess numerical reliability, additional mesh-refinement experiments were carried out using progressively smaller step sizes. The resulting trajectories remained visually indistinguishable under refinement, indicating stable numerical behavior and convergence of the predictor–corrector implementation. These observations are consistent with the theoretical convergence order reported in the literature for the Adams–Bashforth–Moulton method applied to Caputo fractional differential equations.

4.2. Simulation setup and parameters

To illustrate the dynamical behavior of the fractional Lotka–Volterra opinion dynamics model, we simulate the system for several values of the fractional order $q \in (0, 1]$, while keeping the model parameters fixed. This allows us to isolate the influence of the memory parameter q on the transient and asymptotic behavior of the solutions.

Choice of model parameters. The model parameters are chosen as

$$a = 0.7, \qquad b = 0.5, \qquad c = 0.6, \qquad d = 0.8.$$

These values are positive and satisfy the generic condition $a, b, c, d > 0$ required for the theoretical analysis in Section 3. They are not intended to fit any specific empirical dataset but are selected so that the coexistence equilibrium

$$E^* = \left(\frac{d}{c}, \frac{a}{b}\right) = \left(\frac{0.8}{0.6}, \frac{0.7}{0.5}\right) \approx (1.333, 1.4)$$

lies well inside the positive quadrant and is surrounded by a sufficiently large region for clear visualization of the phase portraits and time-series trajectories. This choice is purely illustrative and does not affect the qualitative conclusions regarding the role of the fractional order q.

Fractional orders. To examine the role of fractional memory, we consider the following representative orders:

$$q = 1.0, \qquad q = 0.9, \qquad q = 0.8, \qquad q = 0.7.$$

Here, $q = 1$ corresponds to the classical integer-order Lotka–Volterra system, while $0 < q < 1$ corresponds to the Caputo fractional-order cases.

Initial conditions. For each value of q, trajectories are generated from the following initial conditions in the positive quadrant:

$$(x_0, y_0) = (0.5, 2.0), \qquad (2.0, 0.5), \qquad (1.8, 1.8), \qquad (0.8, 0.8).$$

These initial conditions are distributed on different sides of the coexistence equilibrium to illustrate the qualitative transition from sustained oscillations in the classical case to damped convergence in the fractional cases.

4.3. Numerical results and dynamical interpretation

The numerical simulations presented in Figures 1 and 2 illustrate the stability behavior predicted by the theoretical analysis in Section 3. In particular, they show how the fractional order q affects the transition from persistent oscillations in the classical case to damped trajectories in the fractional-order cases.

4.3.1. Phase portrait analysis

Figure 1 displays the phase portraits of the system for different values of the fractional order q. For the classical integer-order case $q = 1$, the trajectories form closed orbits around the coexistence equilibrium E^*. This behavior is consistent with the neutral stability predicted by the linearization analysis for the classical Lotka–Volterra system.

For fractional orders $0 < q < 1$, the trajectories exhibit inward spiraling behavior toward the coexistence equilibrium E^*. This numerical behavior is consistent with Theorem 3.4, which establishes local asymptotic stability of E^* for $0 < q < 1$ via the Matignon stability criterion. Moreover, the damping effect becomes more pronounced as q decreases. For instance, the case $q = 0.7$ displays stronger contraction toward the equilibrium than the case $q = 0.9$.

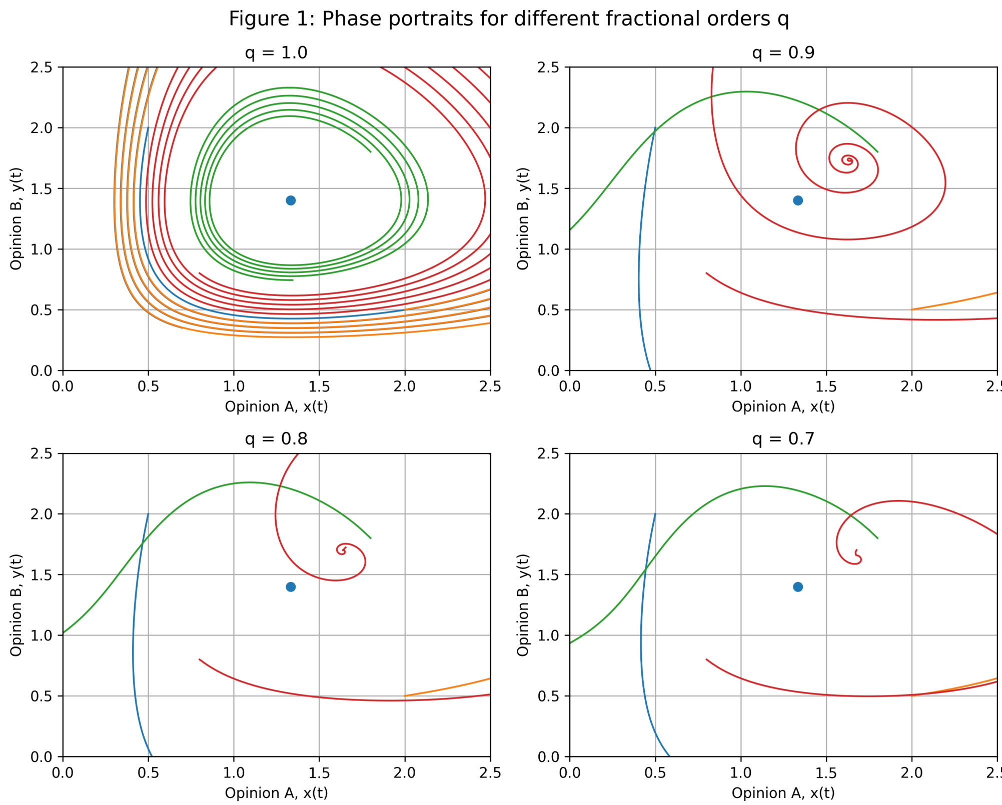

Figure 1. Phase portraits of the fractional-order Lotka–Volterra opinion dynamics model for different values of q. The coexistence equilibrium E^* is marked by a black dot. (a) For $q = 1$, trajectories form closed orbits around E^*, corresponding to the classical neutrally stable behavior. (b) For $q = 0.9$, (c) for $q = 0.8$, and (d) for $q = 0.7$, trajectories spiral inward toward E^*, consistent with the local asymptotic stability result for $0 < q < 1$. The parameter values are $a = 0.7$, $b = 0.5$, $c = 0.6$, and $d = 0.8$, so that $E^* \approx (1.333, 1.4)$. The initial conditions are $(0.5, 2.0)$, $(2.0, 0.5)$, $(1.8, 1.8)$, and $(0.8, 0.8)$. The numerical scheme is the predictor–corrector Adams–Bashforth–Moulton method described in Section 4.1.

4.3.2. Time-series behavior

The time-series plots in Figure 2 provide a complementary view of the transition from sustained oscillations to damped behavior. For $q = 1$, the solution components $x(t)$ and $y(t)$ oscillate around the equilibrium values without visible damping, which is consistent with the center-type behavior of the classical integer-order Lotka–Volterra model.

For $q = 0.9$, $q = 0.8$, and $q = 0.7$, the oscillations decrease gradually over time, and the trajectories approach the coexistence equilibrium

$$(x^*, y^*) \approx (1.333, 1.4).$$

The numerical results indicate that smaller values of q produce stronger damping and faster attenuation of oscillations.

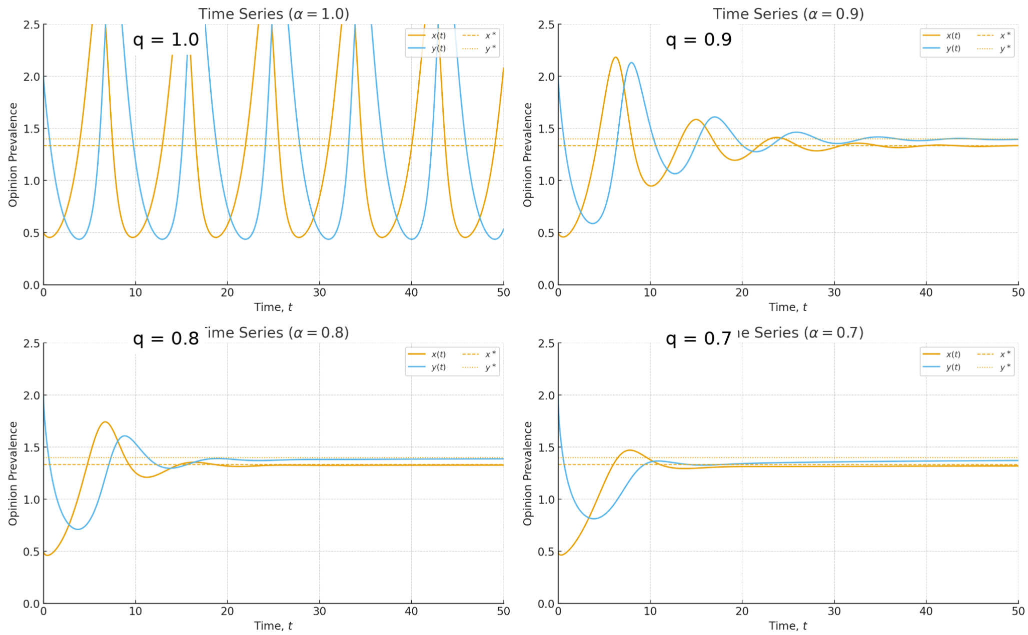

Figure 2. Time-series plots of the opinion prevalences $x(t)$ and $y(t)$ for the initial condition $(x_0, y_0) = (0.5, 2.0)$. (a) For $q = 1$, the solutions exhibit sustained oscillations around the equilibrium. (b) For $q = 0.9$, (c) for $q = 0.8$, and (d) for $q = 0.7$, the oscillations become damped and the solutions approach the equilibrium values $x^* \approx 1.333$ and $y^* \approx 1.4$. The parameter values are $a = 0.7$, $b = 0.5$, $c = 0.6$, and $d = 0.8$. The numerical scheme is the predictor–corrector Adams–Bashforth–Moulton method described in Section 4.1.

4.3.3. Consistency with the stability analysis

The numerical behavior shown in Figures 1 and 2 is consistent with the stability classification established in Section 3. In the classical case $q = 1$, the coexistence equilibrium is neutrally stable and the trajectories remain oscillatory. In contrast, for $0 < q < 1$, the Matignon criterion implies local asymptotic stability of E^*, and the numerical trajectories display damped convergence toward this equilibrium.

From a modeling perspective, these results suggest that the Caputo fractional derivative introduces a memory-dependent damping effect into the competitive opinion dynamics. Thus, within the scope of the present numerical experiments, the fractional-order formulation provides a plausible mechanism for describing gradual stabilization in opinion competition without altering the basic Lotka–Volterra interaction structure.

5. Illustrative calibration using pseudo-temporal prevalence data

The theoretical results of Section 3 and the numerical simulations in Section 4 show that the fractional-order formulation ($0 < q < 1$) introduces a damping mechanism leading to local asymptotic stability of the coexistence equilibrium, whereas the classical integer-order model ($q = 1$) exhibits neutral stability and persistent oscillations. To complement these analytical findings with a purely illustrative numerical exercise, we calibrate both models against a pseudo-temporal prevalence sequence constructed from publicly available data.

5.1. Dataset construction and preprocessing

Critical disclaimer on pseudo-temporal ordering. The dataset used in this section does not contain genuine timestamps. Moreover, the raw CSV file orders tweets by entity, so that tweets associated with the same entity appear consecutively rather than according to any temporal criterion. A direct batch aggregation of the raw file in its original order therefore produces an artificial sequence in which the first batches consist almost exclusively of one entity and the later batches of the other. Consequently, the resulting sequence does **not** reflect real-world temporal dynamics. The analysis presented below is therefore **purely illustrative** and should not be interpreted as a validation of the model against actual opinion dynamics over time. Its sole purpose is to demonstrate the mathematical procedure of fitting the fractional model to a pseudo-temporal prevalence sequence.

Data source. We employ the publicly available Twitter Entity Sentiment Analysis dataset, which consists of short posts labeled by an entity field and associated text content. From this corpus, we select two technology entities, Google and Microsoft, and treat their relative mention prevalence as a proxy for a two-component competitive interaction.

Pseudo-temporal aggregation. Let $\tilde{x}_k$ and $\tilde{y}_k$ denote the raw mention counts of Google and Microsoft, respectively, in the k-th batch. We partition the selected records into K consecutive batches of equal size and set

$$K = 100,$$

thereby obtaining a pseudo-time index $k = 1, 2, \ldots, K$. The choice $K = 100$ is heuristic and was not optimized. Because the raw file is internally ordered by entity rather than by time, this aggregation produces an artificial sequence that does not correspond to a genuine temporal process.

Smoothing. To reduce high-frequency fluctuations caused by the arbitrary batch partitioning, we apply a moving-average filter of window length

$$w = 7$$

in batch units. This yields smoothed signals $\hat{x}_k$ and $\hat{y}_k$. The value $w = 7$ was chosen heuristically to produce a smooth illustrative sequence, and no claim of optimality is made.

Normalization. To align the constructed sequence with the model variables $x(t)$ and $y(t)$, which are interpreted as relative prevalences, we normalize the smoothed signals as

$$x_{\text{data}}(k) = \frac{\hat{x}_k}{\hat{x}_k + \hat{y}_k}, \qquad y_{\text{data}}(k) = \frac{\hat{y}_k}{\hat{x}_k + \hat{y}_k}.$$

Consequently,

$$x_{\text{data}}(k) + y_{\text{data}}(k) = 1, \qquad k = 1, 2, \ldots, K.$$

5.2. Parameter calibration and model fitting

We calibrate both the classical integer-order model ($q = 1$) and the fractional Caputo model ($0 < q < 1$) against the normalized pseudo-temporal sequences

$$\{x_{\text{data}}(k), y_{\text{data}}(k)\}_{k=1}^{K}.$$

The dynamical system used for fitting is

$$
\begin{aligned}
{}^{C}D_t^q x(t) &= ax(t) - bx(t)y(t), \\
{}^{C}D_t^q y(t) &= -dy(t) + cx(t)y(t),
\end{aligned}
$$

where $q \in (0,1]$ and $a, b, c, d > 0$.

The parameter vector

$$\boldsymbol{\theta} = (a, b, c, d, q)$$

is estimated by minimizing the least-squares discrepancy

$$\min_{\boldsymbol{\theta}} \mathcal{I}(\boldsymbol{\theta}) = \frac{1}{K} \sum_{k=1}^{K} \left[\left(x(t_k; \boldsymbol{\theta}) - x_{\text{data}}(k)\right)^2 + \left(y(t_k; \boldsymbol{\theta}) - y_{\text{data}}(k)\right)^2 \right],$$

subject to

$$a > 0, \qquad b > 0, \qquad c > 0, \qquad d > 0, \qquad 0 < q \leq 1.$$

For each candidate parameter set, the model trajectories are generated using the predictor–corrector Adams–Bashforth–Moulton scheme described in Section 4.1.

5.3. Quantitative comparison: RMSE and fit quality

We compare the classical model ($q = 1$) and the fractional model ($0 < q < 1$) using the same pseudo-temporal sequence, the same initial conditions, and the same numerical integration framework.

Since the constructed signals are normalized so that

$$x_{\text{data}}(k) + y_{\text{data}}(k) = 1,$$

we compare them with the model outputs in relative prevalence form:

$$x_{\text{rel}}(t_k) = \frac{x(t_k)}{x(t_k) + y(t_k)}, \qquad y_{\text{rel}}(t_k) = \frac{y(t_k)}{x(t_k) + y(t_k)}.$$

The total root-mean-square error is defined by

$$\text{RMSE} = \sqrt{\frac{1}{K} \sum_{k=1}^{K} \left[\left(x_{\text{rel}}(t_k) - x_{\text{data}}(k)\right)^2 + \left(y_{\text{rel}}(t_k) - y_{\text{data}}(k)\right)^2 \right]}.$$

Table 1 summarizes the fitting results.

Table 1. Quantitative comparison between the classical model and the fractional model for the Google–Microsoft pseudo-temporal prevalence sequence. The fractional model yields a modest reduction in RMSE under the adopted pseudo-temporal aggregation procedure.

Model	Order q	RMSE for x	RMSE for y	Total RMSE
Classical model	1.000	0.02914	0.02914	0.04121
Fractional model	0.787	0.02775	0.02775	0.03924

The reduction in total RMSE from 0.04121 to 0.03924 is modest. Since the underlying pseudo-temporal sequence is artificial and does not represent genuine temporal dynamics, no claim of statistical significance or empirical superiority is made. The comparison is interpreted only as a descriptive numerical illustration.

5.4. Data-to-model comparisons and error curves

Figures 3 and 4 present the data-to-model comparisons for the normalized Google and Microsoft prevalences, respectively. Both formulations can be fitted to the pseudo-temporal sequence. Under the adopted aggregation procedure, the fractional model with $q \approx 0.787$ reproduces the constructed sequence somewhat more closely than the classical model.

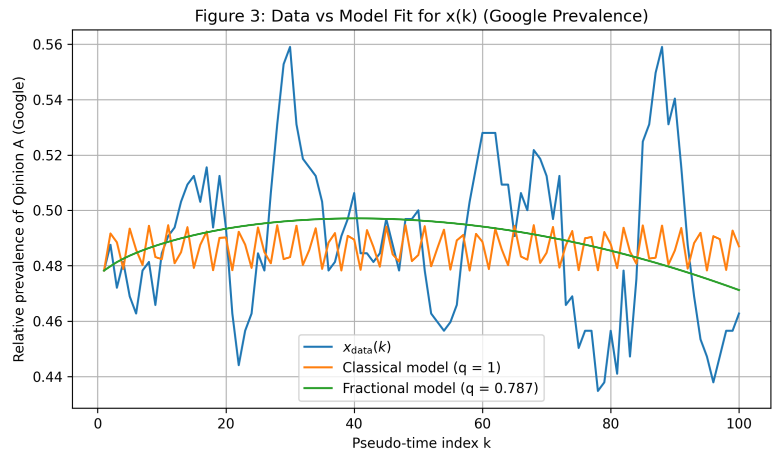

Figure 3. Normalized Google prevalence: Comparison between the pseudo-temporal sequence and model trajectories. Under the adopted aggregation procedure, the fractional model ($q \approx 0.787$) reproduces the constructed sequence somewhat more closely than the classical model ($q = 1$).

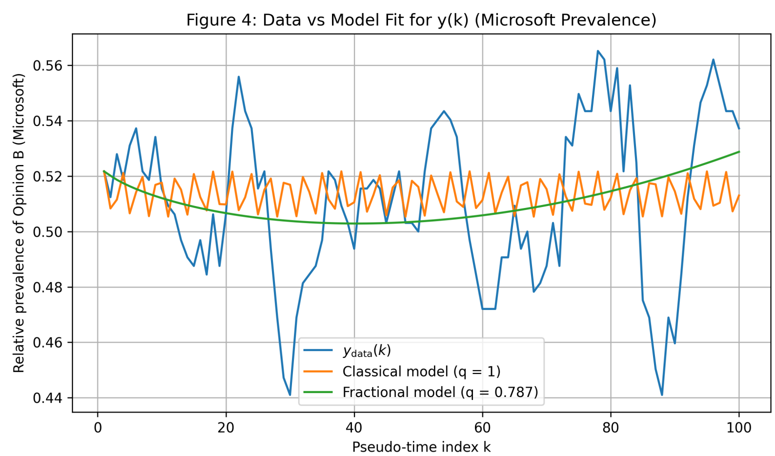

Figure 4. Normalized Microsoft prevalence: Comparison between the pseudo-temporal sequence and model trajectories. The fractional model ($q \approx 0.787$) provides a slightly closer descriptive fit than the classical model ($q = 1$) for the constructed pseudo-temporal sequence.

Figure 5 displays the pointwise Euclidean discrepancy

$$e(k) = \sqrt{(x_{\mathrm{rel}}(t_k) - x_{\mathrm{data}}(k))^2 + (y_{\mathrm{rel}}(t_k) - y_{\mathrm{data}}(k))^2}, \qquad k = 1, 2, \ldots, K.$$

The fractional model gives smaller pointwise errors over much of the artificial index k, which is consistent with the modest reduction in RMSE reported in Table 1.

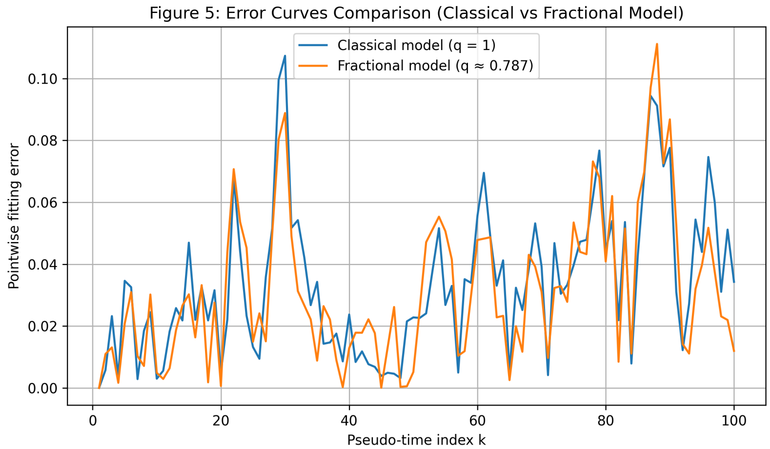

Figure 5. Pointwise error curves $e(k)$ for the classical model ($q = 1$) and the fractional model ($q \approx 0.787$). The fractional model gives smaller errors over much of the pseudo-temporal index under the adopted aggregation procedure.

5.5. Link to the stability theory

The modest quantitative improvement observed for the fractional model on this artificial sequence is consistent with the stability conclusions derived in Section 3. The case $0 < q < 1$ introduces a memory-dependent damping mechanism through the nonlocal structure of the Caputo derivative. In the present illustrative setting, this damping effect allows the fractional model to follow the constructed prevalence transition more smoothly than the classical model, which is associated with neutral stability and persistent oscillatory behavior.

This observation should be interpreted only in a mathematical and descriptive sense. It illustrates how the fractional-order formulation can be fitted to a pseudo-temporal sequence, without implying predictive validity for real-world opinion dynamics.

5.6. Limitations of the illustrative calibration

The following limitations must be emphasized.

- **Absence of temporal information:** The dataset does not contain genuine timestamps. The sequential order in the raw CSV file is determined by entity grouping rather than time. Therefore, the pseudo-temporal sequence constructed by batch aggregation does **not** represent real-world opinion dynamics over time.
- **Artificial aggregation:** The choices $K = 100$ and $w = 7$ are heuristic and were not optimized. The results may depend on these aggregation and smoothing choices.
- **Modest RMSE improvement:** The reduction in total RMSE from 0.04121 to 0.03924 is small and should not be overinterpreted.
- **No statistical testing:** Since the underlying sequence is artificial and does not correspond to a genuine temporal process, formal statistical tests such as p-values or confidence intervals would be potentially misleading. Therefore, no statistical significance test is reported.

- **Illustrative rather than predictive:** This analysis demonstrates the mathematical procedure of calibrating the fractional model to a constructed pseudo-temporal prevalence sequence. It does **not** constitute a validation of the model's predictive power on real opinion dynamics.

6. Conclusion

This study developed a mathematically consistent fractional-order framework for modeling competitive opinion dynamics using a Caputo fractional Lotka-Volterra structure. The analysis began with a rigorous formulation of the system and its equivalent Volterra integral representation, which enabled the establishment of existence and uniqueness of solutions under standard Lipschitz conditions. A comprehensive stability analysis based on the Jacobian linearization and the Matignon criterion demonstrated that the coexistence equilibrium is asymptotically stable for $0 < q < 1$, while the classical integer-order case $q = 1$ exhibits only neutral stability. These theoretical findings were further supported by numerical simulations using a predictor-corrector Adams-Bashforth-Moulton scheme tailored to Caputo fractional derivatives, revealing that the introduction of fractional memory transforms persistent oscillatory behavior into damped convergence toward a stable coexistence state. Finally, an illustrative calibration using normalized pseudo-temporal prevalence data showed that the fractional model achieves a lower root-mean-square error compared to the classical model under the adopted aggregation procedure. In accordance with reviewer comments, we emphasize that this calibration is purely illustrative: The dataset lacks genuine timestamps, the pseudo-temporal aggregation is heuristic, and no claim of statistical significance or predictive validation is made. The limitations of this illustrative component are explicitly discussed in Section 5.

Future research directions naturally arise from both the theoretical and applied perspectives of the proposed framework. On the theoretical side, a rigorous global stability proof via a fractional Lyapunov function and invariant set analysis would further strengthen the dynamical foundations of the model. Extensions to variable-order fractional systems, distributed delays, or multi-agent competitive networks also represent promising avenues for capturing more complex memory-driven social interactions. From an applied standpoint, future work may incorporate higher-resolution time-stamped datasets, stochastic perturbations, and parameter identification under uncertainty to enhance real-world descriptive capability. Moreover, coupling the fractional opinion dynamics model with control mechanisms, such as feedback intervention or adaptive influence strategies, could open new directions in socio-economic policy modeling and data-informed dynamical systems analysis while preserving the mathematical rigor of the fractional calculus framework.

Authors contribution. Conceptualization, methodology: M.A, A.S.; Formal analysis and theoretical investigation: M.A.; Writing–original draft preparation: M.A., A.S.; Writing–review and editing: M.A., A.S.; All authors read and approved the final manuscript.

Funding. This work was supported by the Deanship of Scientific Research, Vice Presidency for Graduate Studies and Scientific Research, King Faisal University, Saudi Arabia [Grant No. KFU264179].

Data availability statement. The dataset used in this study is publicly available from the Kaggle repository Twitter Entity Sentiment Analysis and can be accessed at: https://www.kaggle.com/datasets/jp797498e/twitter-entity-sentiment-analysis?resource=download.

The data were processed and aggregated to construct normalized prevalence time-series for the competing entities analyzed in this work. All data utilized in the validation section are derived from this publicly accessible source, and no proprietary or restricted datasets were used.

Conflict of interest. The authors declare no competing interests.

References

[1] K. I. A. Ahmed, et al., *Analytical solutions for a class of variable-order fractional Liu system under time-dependent variable coefficients*, Results in Physics, 2024, 56, 107311. DOI: 10.1016/j.rinp.2023.107311.

[2] G. Albi, E. Calzola and G. Dimarco, *A data-driven kinetic model for opinion dynamics with social network contacts*, European Journal of Applied Mathematics, 2025, 36(2), 264–290.

[3] N. Almutairi, et al., *A deterministic and stochastic fractional-order model for computer virus propagation with Caputo-Fabrizio derivative: Analysis, numerics, and dynamics*, Computer Modeling in Engineering & Sciences, 2026, 146(3), 1. DOI: 10.32604/cmes.2026.076371.

[4] N. Almutairi and S. Saber, *Application of a time-fractal fractional derivative with a power-law kernel to the Burke-Shaw system based on Newton's interpolation polynomials*, MethodsX, 2024, 12, 102510. DOI: 10.1016/j.mex.2023.102510.

[5] M. Althubyani, et al., *Epidemiological modeling of pneumococcal pneumonia: Insights from ABC fractal-fractional derivatives*, Computer Modeling in Engineering & Sciences, 2025, 143(3), 3491. DOI: 10.32604/cmes.2025.061640.

[6] K. Cao and Y. Chen, *Fractional Order Crowd Dynamics: Cyber-Human System Modeling and Control*, Vol. 4, Walter de Gruyter GmbH & Co. KG, 2018.

[7] C. Castellano, S. Fortunato and V. Loreto, *Statistical physics of social dynamics*, Reviews of Modern Physics, 2009, 81(2), 591–646.

[8] D. Centola, *The spread of behavior in an online social network experiment*, Science, 2010, 329(5996), 1194–1197.

[9] P. Clifford and A. Sudbury, *A model for spatial conflict*, Biometrika, 1973, 60(3), 581–588.

[10] A. K. S. Dalbon, E. N. D. Rao, K. S. Reddy and A. S. Ram, *Challenges and sustainability of contiguous mining leases in India: Legal, environmental, and socio-economic perspectives from Goa, Karnataka, and Odisha states*, Social Sciences & Humanities Open, 2026, 13, 102426.

[11] K. Diethelm, N. J. Ford and A. D. Freed, *A predictor-corrector approach for the numerical solution of fractional differential equations*, Nonlinear Dynamics, 2002, 29(1), 3–22.

[12] V. D. Djordjevic, J. Jarić, B. Fabry, J. J. Fredberg and D. Stamenović, *Fractional derivatives embody essential features of cell rheological behavior*, Annals of Biomedical Engineering, 2003, 31(6), 692–699.

[13] D. S. Evans and R. Schmalensee, *Matchmakers: The New Economics of Multisided Platforms*, Harvard Business Review Press, 2016.

[14] S. Galam, *Sociophysics: A Physicist's Modeling of Psycho-Political Phenomena*, Springer US, 2011.

[15] R. Garrappa, *Numerical solution of fractional differential equations: A survey and a software tutorial*, Mathematics, 2018, 6(2), 16.

[16] S. He, H. Wang and K. Sun, *Solutions and memory effect of fractional-order chaotic system: A review*, Chinese Physics B, 2022, 31(6), 060501.

[17] D. Helbing, *Social Self-Organization: Agent-Based Simulations and Experiments to Study Emergent Social Behavior*, Springer, 2012.

[18] P. Holme and J. Saramäki, *Temporal networks*, Physics Reports, 2012, 519(3), 97–125.

[19] L. Huang, D. F. Xie, L. Li and Z. He, *A survey on data-driven modeling of human drivers' lane-changing decisions*, arXiv preprint, 2025. arXiv:2505.06680.

[20] E. Ising, *Beitrag zur Theorie des Ferromagnetismus*, Zeitschrift für Physik, 1925, 31(1), 253–258.

[21] H. Jafari, R. M. Ganji, N. S. Nkomo and Y. P. Lv, *A numerical study of fractional order population dynamics model*, Results in Physics, 2021, 27, 104456.

[22] G. Jin, H. Fan, Y. Wu, Y. Shi, Y. Fang, J. Zhang and Y. Liang, *A Survey on Sociophysics-Guided Deep Learning for Social Dynamics: Taxonomy, Methods, and Outlook*, Methods, and Outlook, 2026.

[23] M. Kenney and J. Zysman, *The rise of the platform economy*, Issues in Science and Technology, 2016, 32(3), 61.

[24] A. A. Kilbas, H. M. Srivastava and J. J. Trujillo, *Theory and Applications of Fractional Differential Equations*, Vol. 204, Elsevier, 2006.

[25] S. A. Kiselev, A. A. Podberezkin, A. M. Borzenkov, A. V. Ostroukh and C. B. Pronin, *Dynamic pricing in air cargo: Machine learning and genetic algorithm-based optimization*, in 2025 Wave Electronics and its Application in Information and Telecommunication Systems (WECONF), IEEE, 2025, 1–5.

[26] J. Lee, J. Kang, S. Son and H. M. Oh, *Numerical weather data-driven sensor data generation for PV digital twins: A hybrid model approach*, IEEE Access, 2025, 13, 5009–5022.

[27] Y. Lin, J. Tang, J. Guo, S. Wu and Z. Li, *Advancing AI-enabled techniques in energy system modeling: A review of data-driven, mechanism-driven, and hybrid modeling approaches*, Energies, 2025, 18(4), 845.

[28] A. J. Lotka, *Elements of Physical Biology*, Williams & Wilkins, 1925.

[29] J. T. Machado, V. Kiryakova and F. Mainardi, *Recent history of fractional calculus*, Communications in Nonlinear Science and Numerical Simulation, 2011, 16(3), 1140–1153.

[30] C. Magazzino, T. Gattone and M. Madaleno, *The impact of socio-economic factors on the ecological footprint in Turkey: A comprehensive analysis using machine learning approaches*, Journal of Environmental Management, 2025, 387, 125861.

[31] R. L. Magin, *Fractional Calculus in Bioengineering*, Begell House Publishers, 2006.

[32] F. Mainardi, *Fractional Calculus and Waves in Linear Viscoelasticity: An Introduction to Mathematical Models*, World Scientific, 2022.

[33] D. Matignon, *Stability results for fractional differential equations with applications to control processing*, in Proceedings of the IMACS Multiconference on Computational Engineering in Systems Applications (CESA'96), Lille, France, 1996, 963–968.

[34] R. Metzler and J. Klafter, *The random walk's guide to anomalous diffusion: A fractional dynamics approach*, Physics Reports, 2000, 339(1), 1–77.

[35] P. S. Meyer and J. H. Ausubel, *Carrying capacity: A model with logistically varying limits*, Technological Forecasting and Social Change, 1999, 61(3), 209–214.

[36] T. Modis, *Technological forecasting at the stock market*, Technological Forecasting and Social Change, 1999, 62(3), 173–202.

[37] J. Mou, X. Chen, W. Du and J. Han, *Simulation research on the optimization of rural tourism system resilience based on a long short-term memory neural network—Taking well-known tourist villages in Heilongjiang Province as examples*, Sustainability, 2025, 17(3), 1305.

[38] B. I. A. Muttaqin and C. N. Rosyidi, *Open pit mining profit maximization considering selling stage and waste rehabilitation cost*, in AIP Conference Proceedings, AIP Publishing LLC, 2017, 1902(1), 020022.

[39] K. Oldham and J. Spanier, *The Fractional Calculus Theory and Applications of Differentiation and Integration to Arbitrary Order*, Vol. 111, Elsevier, 1974.

[40] K. M. Owolabi, J. F. Gómez-Aguilar and B. Karaagac, *Modelling, analysis and simulations of some chaotic systems using derivative with Mittag-Leffler kernel*, Chaos, Solitons & Fractals, 2019, 125, 54–63.

[41] A. De Paola, L. Fortunati, E. Musiari, G. P. Anselmi, D. Curro, N. Andreadou and G. Fulli, *Residential load forecast: An enhanced machine learning model with socio-economic data and synthetic features*, Results in Engineering, 2026, 109184.

[42] A. P. Parizad, E. Dehghani and M. A. M. A. Kermani, *Data driven framework for ranking influential nodes in social networks using machine learning and neural networks*, Social Network Analysis and Mining, 2026, 16(1), 13.

[43] G. G. Parker, M. W. Van Alstyne and S. P. Choudary, *Platform Revolution: How Networked Markets are Transforming the Economy and How to Make Them Work for You*, WW Norton & Company, 2016.

[44] I. Podlubny, *Fractional Differential Equations: An Introduction to Fractional Derivatives, Fractional Differential Equations, to Methods of Their Solution and Some of Their Applications*, Vol. 198, Elsevier, 1998.

[45] G. Ren, Y. Yu, Z. Lu and W. Chen, *A fractional order model for rumor spreading in mobile social networks from a stochastic process*, in 2021 9th International Conference on Systems and Control (ICSC), IEEE, 2021, 312–318.

[46] K. Sastry, D. E. Goldberg and G. Kendall, *Genetic algorithms*, in Search Methodologies: Introductory Tutorials in Optimization and Decision Support Techniques, Springer US, 2013, 93–117.

[47] D. S. Seara, J. Colen, M. Fruchart, Y. Avni, D. G. Martin and V. Vitelli, *Sociohydrodynamics: Data-driven modeling of social behavior*, Proceedings of the National Academy of Sciences, 2025, 122(35), e2508692122.

[48] A. Sirbu, V. Loreto, V. D. Servedio and F. Tria, *Opinion dynamics: Models, extensions and external effects*, in Participatory Sensing, Opinions and Collective Awareness, Springer International Publishing, 2016, 363–401.

[49] E. Solouma, et al., *On the stochastic simulation by optimal control and bifurcation analysis of the computer virus model in Caputo-type*, Alexandria Engineering Journal, 2026, 144, 12–22. DOI: 10.1016/j.aej.2026.04.017.

[50] V. E. Tarasov, *Fractional nonlinear dynamics of learning with memory*, Nonlinear Dynamics, 2020, 100(2), 1231–1242.

[51] V. Volterra, *Variazioni e fluttuazioni del numero d'individui in specie animali conviventi*, Società Anonima Tipografica "Leonardo da Vinci", 1926.

[52] S. Wang, S. Bekiros, A. Yousefpour, S. He, O. Castillo and H. Jahanshahi, *Synchronization of fractional time-delayed financial system using a novel type-2 fuzzy active control method*, Chaos, Solitons & Fractals, 2020, 136, 109768.

Received February 2026; Accepted July 2026; Available online August 2026.